

Removal of the Methylene Blue Dye (MB) with Catalysts of Au-TiO₂: Kinetic and Degradation Pathway

María-Cruz Arias¹, Claudia Aguilar^{1*}, Mohamad Piza¹, Elvira Zarazua², Francisco Anguebes¹, Víctor Cordova¹

¹Faculty of Chemistry, Autonomous University of Carmen, City of Carmen, Mexico

²Department of Ecomaterials and Energy, Autonomous University of Nuevo León, San Nicolás de los Garza, México

Email: *caguilar@pampano.unacar.mx

How to cite this paper: Arias, M.-C., Aguilar, C., Piza, M., Zarazua, E., Anguebes, F. and Cordova, V. (2021) Removal of the Methylene Blue Dye (MB) with Catalysts of Au-TiO₂: Kinetic and Degradation Pathway. *Modern Research in Catalysis*, 10, 1-14. <https://doi.org/10.4236/mrc.2021.101001>

Received: November 19, 2020

Accepted: January 26, 2021

Published: January 29, 2021

Copyright © 2021 by author(s) and Scientific Research Publishing Inc. This work is licensed under the Creative Commons Attribution International License (CC BY 4.0).

<http://creativecommons.org/licenses/by/4.0/>



Open Access

Abstract

Au-TiO₂ catalysts were used in the photocatalytic degradation of the methylene blue dye (MB). The synthesis of titanium oxide (TiO₂) was carried out by sol-gel method. Subsequently, particles of Au were deposited on the surface of the semiconductor by photo-deposition, thus modifying the surface of the semiconductor. For the characterization of the catalyst obtained, the techniques of X-ray Diffraction (DRX), Scanning Electron Microscopy (SEM), Spectroscopy with Diffuse Reflectance (DR) and Surface Area by the BET (Brunauer, Emmett y Teller) were used. The solid obtained was tested experimentally as a catalyst in the photocatalytic degradation of a solution of MB. The data obtained were analyzed by UV-vis Spectroscopy and Total Organic Carbon (TOC) and the results indicated conversions were greater than 80%. The intermediate products were evaluated by mass coupled gas chromatography (GC-MS) and the MB decomposition route was by hydroxylation, obtaining aromatic intermediates, esters and products of the chemical degradation of the molecule.

Keywords

Titanium Oxide, Water Pollution, Methylene Blue Dye, Heterogeneous Photocatalysis

1. Introduction

The contamination of the water generates a great concern, due to the increase in the demand for drinking water due to the exponential growth of the population [1]. The pollutants that represent a challenge in water treatment are organic, since

their behavior depends on their structure, size, shape or presence of functional groups that determine their toxicity. Within this type of pollutants, there are persistent and recalcitrant ones; both harmful to the environment and human health.

The recalcitrant pollutants also tend to be difficult to degrade since they resist the attack of microorganisms or biological or chemical degradation mechanisms; therefore, it is necessary to make use of Advanced Oxidation Technologies (AOTs), either as a pre-treatment before a biological treatment for biodegradation-resistant contaminants or as a post-treatment process to improve the water before discharge to the receiving bodies [2].

Dyes are used by many industries to color their products (textile, tannery, paper and pulp, cosmetics, plastics, coffee pulp, pharmaceutical, food processing, among other industries) [3] [4]. Of all these industries, the textile ranks first in the use of dyes to dye fibers [4]. Many of these dyes have entered water bodies and have become a threat to the environmental safety of water [5]. Acute exposure to MB causes increased heart rate, skin irritation, Heinz body formation, cyanosis, jaundice, quadriplegia, and tissue necrosis in humans [6] [7].

Although several physical and chemical processes have been adopted, such as sedimentation [8], oxidation by ozone and hypochlorite [9], precipitation, adsorption (by activated carbon), air extraction, coagulation, reverse osmosis, ion exchange, and membrane nanofiltration to the removal of organic pollutants [10]; the application of these methods is restricted due to high cost and low degradation efficiency.

Photocatalysis has proven to be an efficient method to remove organic molecules in non-toxic and biodegradable end products [11]. Photocatalytic activation is a process by which a semiconductor material absorbs light of energy greater than (or equal to) its band gap. Electron-hole pairs are generated by excitations of electrons from the valence band to the conduction band. Such pair formation generates free radicals such as hydroxyl groups ($\cdot\text{OH}$) in the system, which are very efficient oxidants of organic materials [12].

Different semiconductor photocatalysts, such as TiO_2 , ZnO , SrTiO_3 , ZnS , CdS and ZrO_2 have been used for the degradation of contaminants [13] [14]. One of the main drawbacks of photocatalytic activity is the rapid recombination of photoinduced electron-hole pairs. To overcome the inconveniences and improve the photocatalytic activity, the semiconductors are modified with metals. Doping is a very useful technique to improve load separation in the semiconductor system [10]; the semiconductor doping approach is considered as the most efficient way to improve your photocatalytic activity under sunlight [15].

The TiO_2 have attracted extensive interest as promising material in environmental pollution abatement [16], it is a low-cost metal oxide photocatalyst, biocompatible, highly available and stable in the environment with the ability to effectively degrade a spectrum of pollutants [17] [18].

Due to its many advantages, TiO_2 is the main semiconductor used in photo-

catalytic processes; however, this oxide has some limitations related to the greater recombination of the holes and electrons [19]. To remedy this effect, TiO₂ is generally associated with other materials that decrease the recombination rate of electrons and holes, allowing these charges to be transferred to electron acceptors and donors [20] [21]. Particularly, gold nanoparticles have been used as photocatalysts in the degradation of dyes [22] [23]. For these reasons, researchers have recently focused on supporting gold nanoparticles on titanium dioxide, which is a promising system for photocatalytic reactions and wastewater treatment.

This study shows the efficiency of doped catalysts with MB, it is shown that the photocatalytic processes are highly efficient to remove certain organic molecules and that the efficiency of the process depends on the method of synthesis of the solid and the Nature of the contaminant.

2. Experimental

2.1. Materials

The catalyst was synthesized from the Titanium butoxide (Aldrich CAS number: 5593-70-4). Was used methylene blue (Hycel CAS number: 7220-79-3) to simulate an effluent in the photodegradation tests; on the other hand the source of Au was the H₂AuCl₄ (Aldrich CAS number: 16961-25-4). The separation of the catalyst of the solution is carried out by using cellulose filters of 0.22 μm (Millipore-Corp).

2.2. Catalysts Preparation

Synthesis process: The deionized water and the anhydrous ethanol were mixed in a 500 mL glass reactor and the mixture was stirred for one hour. The solution was heated at 70 °C while the titanium butoxide was slowly added, keeping the pH = 3, with the addition of drops of HNO₃, diluted 1:10 in volume. After the addition, a condensation system was placed and the heating and stirring conditions were maintained for 6 hours. The product was dried at 100 °C for 60 min and calcined at 550 °C for 3 hours.

2.2.1. Catalysts Doping

Particles of Au were deposited on the surface of the semiconductor by Photodeposition method using as a precursor H₂AuCl₄·3H₂O. To perform the process in a glass reactor, 1 g of TiO₂ was deposited, 8 mL of ethanol and 100 mL of deionized water were added. It was left one hour in the dark, and the reaction was subjected to the radiation of 4 UV lamps at 365 nm for 5 h. At the end of the irradiation period, water was removed by vacuum filtration followed by drying at 100 °C and calcination at 550 °C for 3 h.

2.2.2. Characterization by XRD, EDS, BET and DR

The characterization of the synthesized materials allows to establish their structural properties. XRD diffraction pattern was obtained with Advance D8 Dif-

fractometer. The morphology of the samples and chemical analysis were studied using a Dual-Beam Scanning Electron Microscope (FIB-SEM) FEI-Helios Nanolab 600 from National Laboratory of Research in Nanosciences and Nanotechnology (LINAN, San Luis Potosí, México).

The band gap estimation (E_g) was analyzed by UV-vis spectroscopy by DR using a Shimadzu UV-2450 system, equipped with the ISR-2200 Integrating Sphere Attachment (UASLP, Autonomous University of San Luis Potosí, México). BET surface area and porosity measurements were carried out by N_2 adsorption at 77 K using a BelCorp II instrument from Civil Engineering Institute (UANL, Autonomous University of Nuevo León, México).

2.3. Photocatalytic Degradation of MB

The catalyst was evaluated in the degradation of MB at different concentrations, with the purpose of knowing the effect of the concentration of the substrate on the degradation velocity. Thus, in all the photoactivity tests, samples were taken to determine the advance grade of the reaction. The decrease of MB concentration in the solution was determined by monitoring the intensity of its principal absorption band (664 nm) in an Agilent Cary 60 spectrophotometer (UNACAR, Autonomous University of Carmen, México).

2.4. GC-MS

Reaction samples were treated with ethylacetate and Micro Extraction in Solid Phase (SPEM) with LiChrolut® Florisil® cartridges, and then analyzed using GC-MS was used an equipment HP model 6890 coupled to a selective mass detector HP 5973. A column HP-5MS 25 m \times 0.2 mm \times 0.33 μ m and Helium of high purity as carrier gas, the temperature program was as follows: initial temperature of 40°C, at 2 minutes the heating ramp of 10°C min⁻¹ begins until reaching 260°C, which is maintained for 45 minutes. The injector is used in “*Splitless*” mode at 250°C. The NIST Version 1.7a electronic library data base was used to assign the identified peaks.

3. Results and Discussion

3.1. XRD

XRD patterns of the TiO_2 y $Au-TiO_2$ are presented in **Figure 1**. The samples confirm the presence of anatase of titania (JPDF 211272). The highest diffraction peak in 2θ , for the anatase phase, occurs at 25.42° further the XRD patterns of $Au-TiO_2$ have peaks at $2\theta = 38.15^\circ$, 44.29° , 64.54° and 77.58° (JPDF XRD 893697), this as a result of the gold with which the materials have been doped. The presence of the anatase phase in a higher proportion can be attributed to the synthesis method and the temperature at which the process is carried out; with reflections of $2\theta = 37.8$, 48, 53.9 and 63 corresponding to the crystallographic planes of 004, 200, 105, 204 based on the JCPDS 21-1272 pattern. In previous

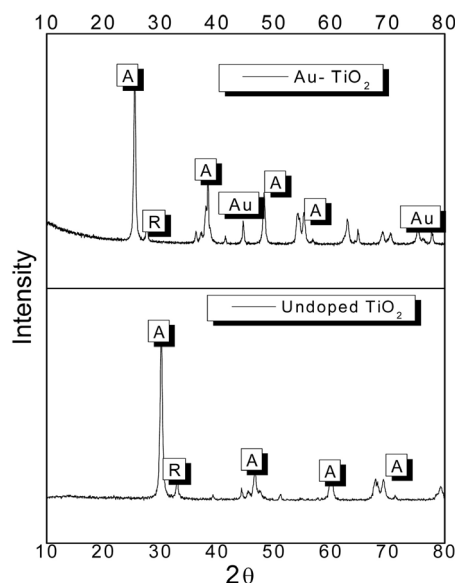


Figure 1. XRD of TiO₂ and Au-TiO₂.

studies [24]. It has been shown that at temperatures of 400°C the crystalline phase of anatase occurs in a greater proportion, when the calcination temperature is increased to 600°C, anatase is uniquely observed; reflections belonging to rutile were detected in undoped titania. Doping with gold can influence in delaying the transition from the crystalline phase to anatase from the XRD patterns, the peaks shift to lower angle after Au deposition, which may indicate the increase of the cell volume which can be attributed changes in composition by doping. This effect is mainly due to the difference in ionic radii between the main element and the dopant ion, if we modify the original system by using a dopant, it affects the lattice/unit cell of the material, change in lattice parameters result in shift in XRD peaks. The dopant atoms are being taken into the host structure substituting for some of the host atoms and thus causing the structure to either contract or expand.

3.2. SEM-EDS

Figure 2 shows the micrographs obtained from the solid sample of Au-TiO₂ in which the morphological characteristics of the materials are exemplified, in addition to showing a uniform distribution of the gold particles. The chemical composition of the Au-TiO₂ was determined by energy dispersive spectroscopy (EDS) analysis, obtaining Ti = 53.17%, Au = 3.7% and O = 43.17.

Figure 3 shows the modifications of the properties of titanium oxide due to the presence of gold particles on the surface. A significant improvement in absorption due to surface plasmon resonance in visible light range was achieved (400 - 600 nm), resulting from the interaction of the metal particles with the incident light. Likewise, the presence of metallic elements can increase the properties and electrical conductivity of a semiconductor when it is doped [25]. The obtained results indicate that the band gap energy of the titanium modified with

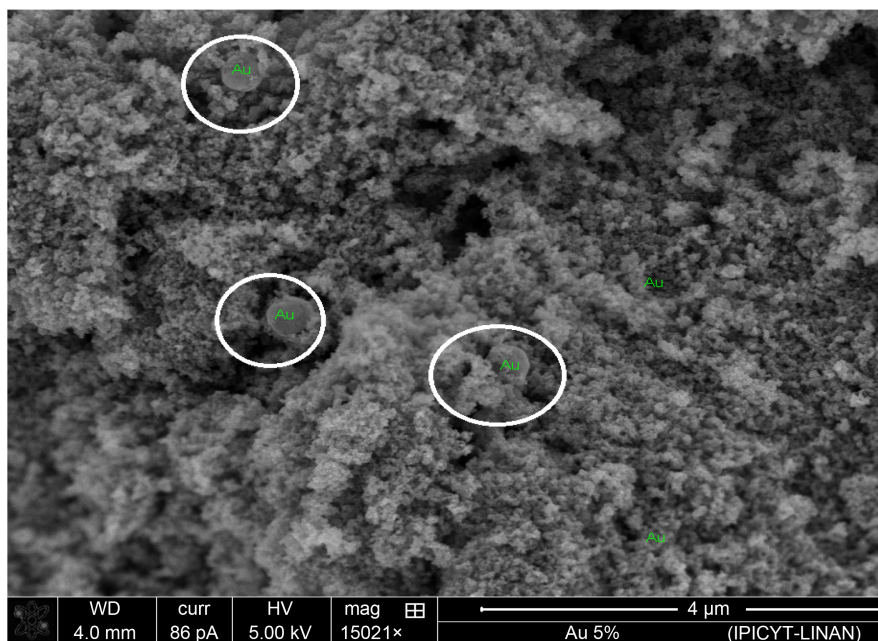


Figure 2. SEM image showing the elemental composition of the synthesized catalyst.

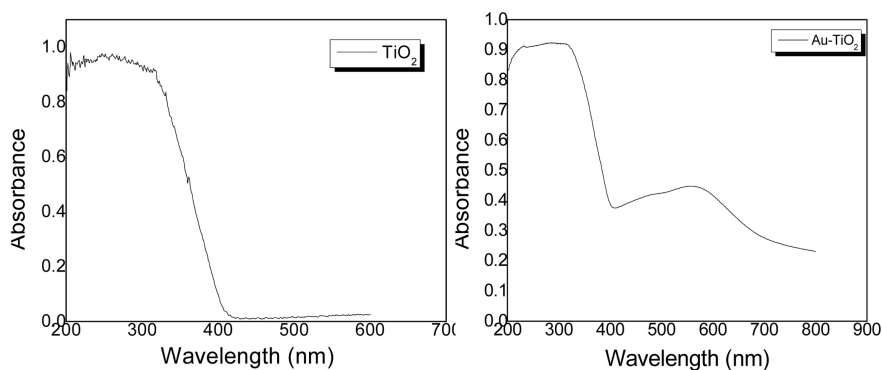


Figure 3. Comparison of the diffuse reflectance profiles of TiO_2 and Au-TiO_2 .

gold was 2.9 eV, compared to commercial TiO_2 which is 3.1.

3.3. BET

The N_2 adsorption-desorption isotherms of the synthesized Au-TiO_2 samples are presented in **Figure 4**. The isotherms of the catalyst follow type IV adsorption-desorption characteristics of (IUPAC; International Union of Pure and Applied Chemistry) classification which indicates uniform size and mesoporous structure of the sample. Specific surface area is $47.57 \text{ m}^2/\text{g}$, an average pore radius of 30.668 nm, and a total pore volume of $0.3648 \text{ cm}^3/\text{g}$.

3.4. Photocatalytic Degradation of MB

The mass of the catalyst used was 1 g/L; this relationship was based on previous studies carried out in the research group.¹ **Figure 5** shows the concentration profile of an MB photocatalytic degradation reaction at a concentration of 10

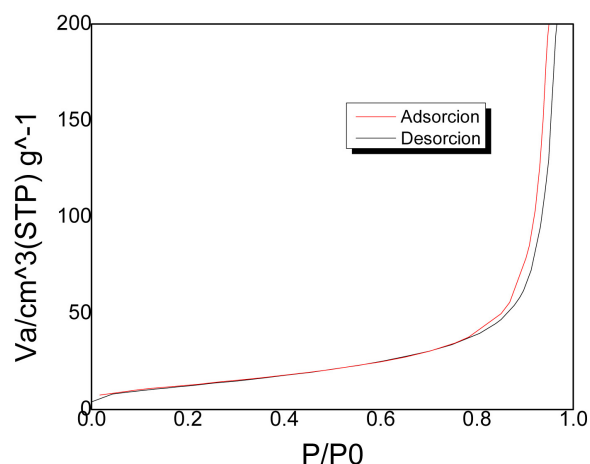


Figure 4. N₂ adsorption-desorption isotherms of Au-TiO₂.

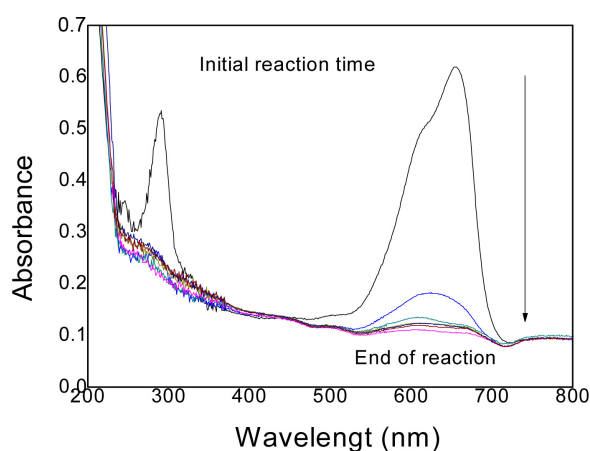


Figure 5. Degradation profile of MB of a 10 mg/L MB solution.

ppm. As can be seen, the absorption spectra of MB indicate most intense absorption peak at 664 nm, which has been associated to MB monomer, the conjugation system between the two-dimethylamine substituted aromatic rings through sulfur and nitrogen atoms. During photocatalytic degradation, the intensity of this peak decrease gradually.

This experiment was carried out in dye solutions of 5, 10, 15, 20, 25, 30, 35, 40, 45 and 50 ppm. **Table 1** shows the degradation percentages obtained of all the reactions and **Figure 6** shows the decrease in the concentration of the dye vs. time, the greatest conversion is obtained with the 30 mg/L solution with a 97.4%.

In all degradation reactions of MB, samples of the reaction mixture were taken for analysis with UV-vis and TOC. The results of these experiments are showed in the **Figure 6**, where the variation of the concentration of MB and the total amount of organic carbon can be observed as a function of the time.

The degradation of MB, measured by UV-vis spectroscopy, and a mass balance, based on total organic carbon measurements were used to obtain the average Organic intermediate products (OIP) curve using the equation:

Table 1. Degradation percentage of the analyzed samples.

Concentration (mg/L)	Conversionpercentage (%)
5	88.6
10	92.5
15	93.9
20	94
25	95.8
30	97.4
35	92.5
40	93.2
45	95.2
50	96.7

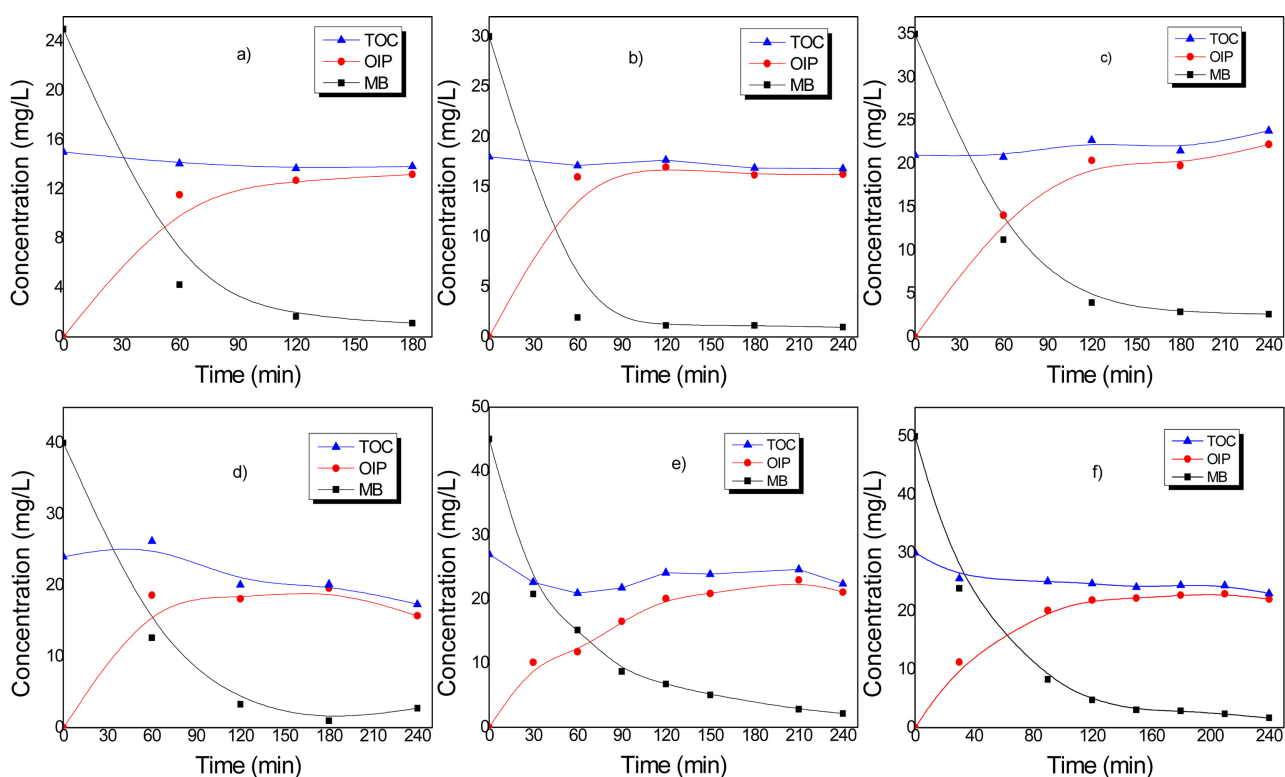


Figure 6. Methylene blue (MB) concentration profile at different reaction times: (a) 25 mg/L, (b) 30 mg/L, (c) 35 mg/L, (d) 40 mg/L, (e) 45 mg/L, (f) 50 mg/L showing the reaction behavior based on mass balances and total organic carbon profiles (TOC = total organic carbon, MB = concentration measured by UV-vis spectroscopy, OIP = organic intermediate products).

$$\text{TOC} - C_{\text{CARBON}} \text{MB} = C_{\text{CARBON}} \text{OIP} \quad (1)$$

The Langmuir-Hinshelwood (LH-HW) model is the most commonly used kinetic expression to explain the kinetics of heterogeneous catalytic reactions. In this model, the reaction rate r can be expressed as:

$$-r_{\text{MB}} = -\frac{dC_{\text{MB}}}{dt} = \frac{K_1 C_{\text{MB}}}{1 + K_2 C_{\text{MB}}} \quad (2)$$

where K_1 is a rate constant, K_2 is the adsorption constant, and C_{MB} is the methylene blue concentration (**Figure 7**).

The Equation (2) allows to graph the experimental data for determine the values of the constants. The correlation coefficient (R^2) for the fitted straight line was calculated as 0.9852, suggesting that the photocatalytic degradation of MB can be described by a first-order kinetic model. The obtained values were as follows: $K_1 = 0.00670736 \text{ min}^{-1}$, $K_2 = 0.01066067 \text{ (Mg / L)}$ raised to -1 .

3.5. Intermediate Organic Products of MB Degradation

Samples were analyzed at two and four hours of reaction that were extracted by SPEM and analyzed by GC-MS (2 and 6 hours of reaction). The reaction samples were extracted by SPEM and analyzed by GC-MS. The results are shown in **Figure 8** and **Figure 9** respectively. The results obtained indicate that the degradation pathway is hydroxylation; The first intermediate was 1, 2, 3, 4 Tetramethyl benzene shown in **Figure 8(c)** with a retention time TR = 6.941, the reaction can proceed in series or in parallel, The structure of MB has an aromatic ring opening with the subsequent formation of compounds with an open structure, which can give rise to Triethanolamine shown in **Figure 8(d)** with a TR = 6.653, finally the subsequent oxygenation of the MB molecule can lead to the formation of carboxylic acids or esters such as those seen in **Figure 8(b)** and **Figure 8(a)** with TR = 16.72 (Hexadecanoic acid, methyl ester) respectively, it was not possible to identify all the intermediates since the speed at which they are formed and consumed can be nanoseconds, but it is a fact that it is a aromatic ring opening and ester formation; In other investigations [26]; The behavior showed a rapid removal of color, TiO_2 -UV-based photocatalysis was able to simultaneously oxidize the dye, with an almost complete mineralization of carbon and nitrogen and sulfur heteroatoms in CO_2 , NH_4^+ , NO_3^- and SO_4^{2-} respectively.

Finally in **Figure 9(a)** and **Figure 9(b)**; fragments of the MB molecule can be observed, product of the degradation of the chemical structure with TR = 1.564 (Methylene chloride) and TR = 1.719 (2-butanone).

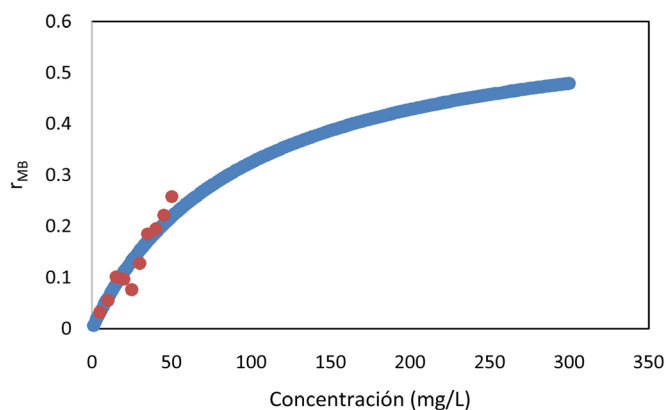


Figure 7. Experimental data on Langmuir–Hinshelwood model (LH equation).

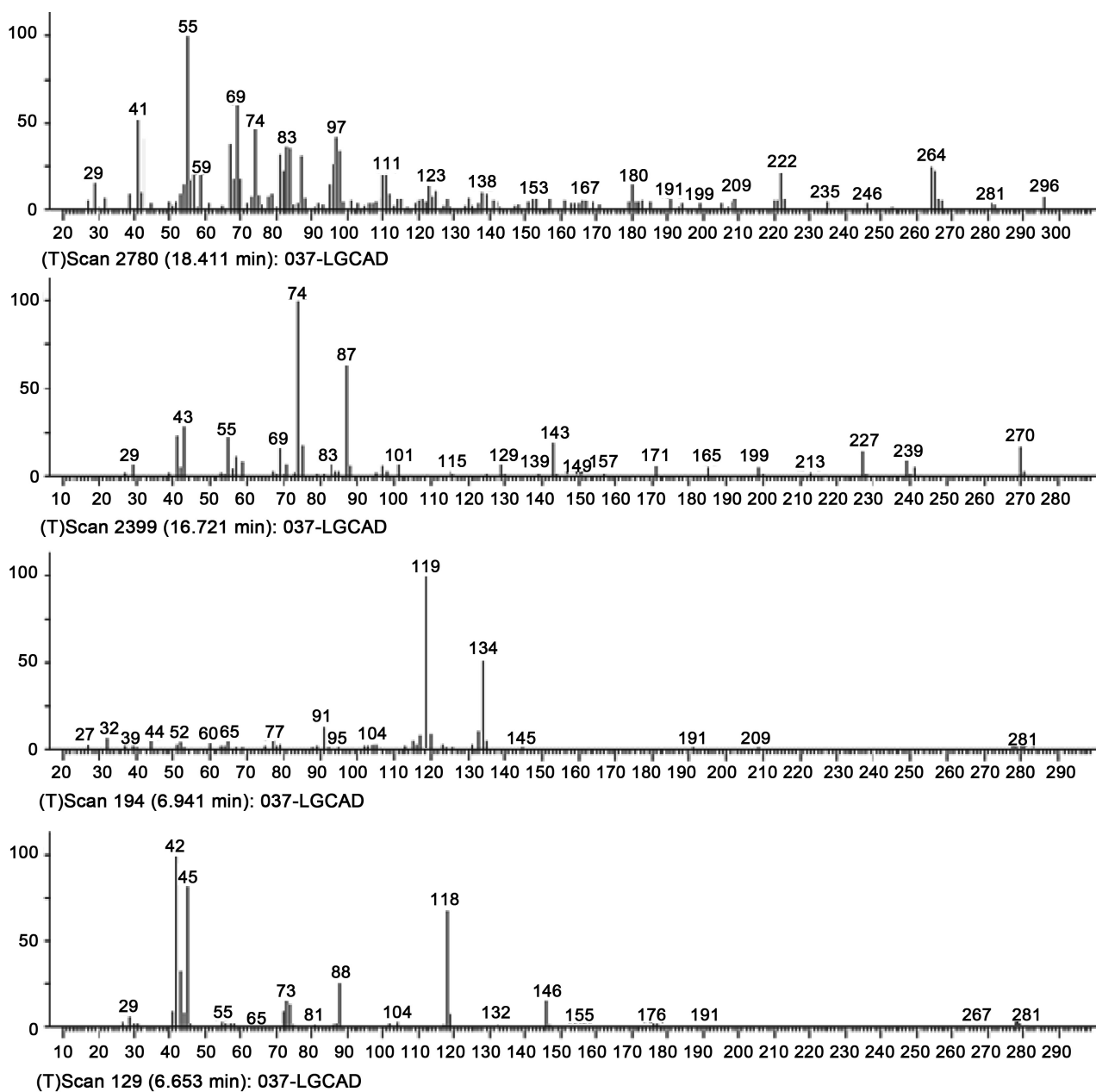


Figure 8. GC-MS spectra of MB degradation at 2 hours of reaction (four peaks are identified with retention times in minutes (a) 18.41; (b) 16.721; (c) 6.941; (d) 6.653).

Two oxidative agents can be obtained from the photocatalytic process: the photo-produced holes h^+ and/or the $\cdot OH$ radicals, which are known as strongly active and degrading but non-selective agents, the $\cdot OH$ radicals can attack the $C-S^+=C$ functional group in MB. Thus, the initial step of MB degradation can be attributed to the cleavage of these bonds to obtain degradation of the dye [23]. Due to breaking of bonds during a reaction time of 2 hours a single ring structure of 1, 2, 3, 4. Tetramethyl benzene is produced at 6.941 retention time. Ray *et al.* [27] suggest that multiple single ring structures are produced. Finally, the organic compounds are mineralized during a reaction time of

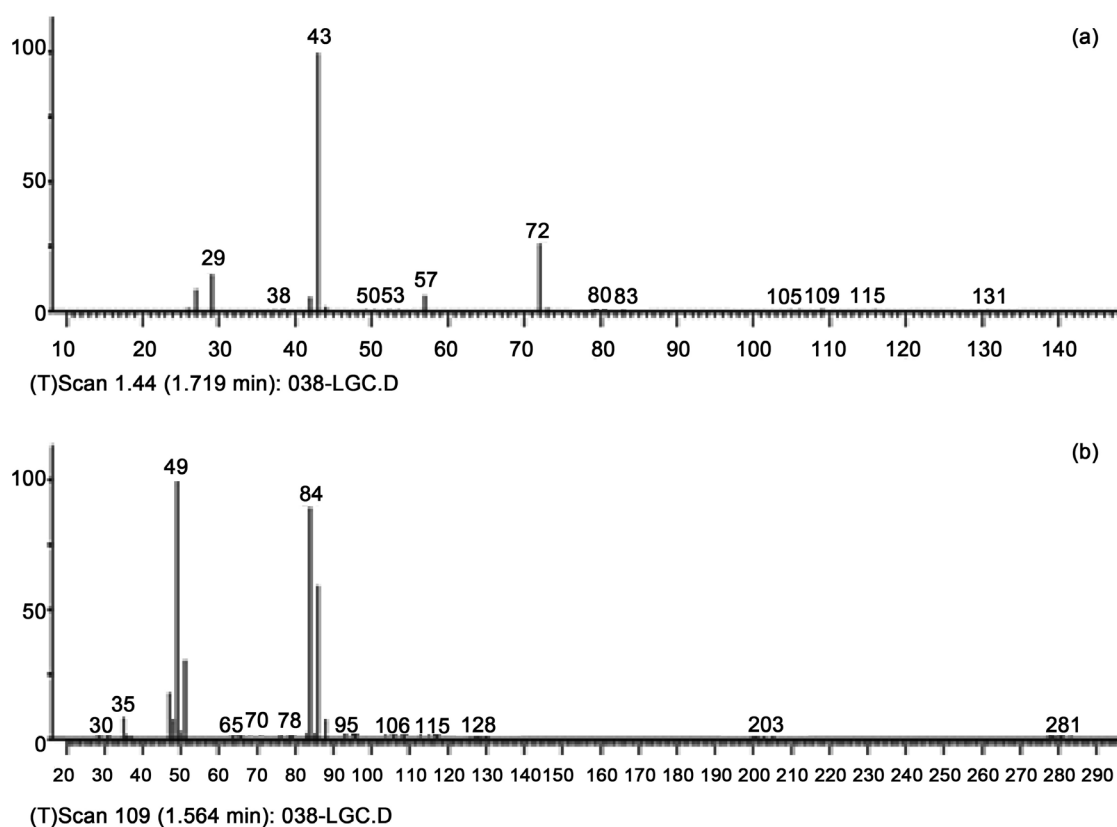


Figure 9. GC-MS spectra of the degradation of MB at 4 hours of reaction (2 peaks are identified with retention times in minutes of (a) 1.719 min; (b) 1.5654 min).

6 hours in methylene chloride and 2-butanone. Houas *et al.* [23] have mentioned on their study that many other hydroxylated intermediates have been formed of the degradation of methylene blue, but they were difficult to detect because of their poor extractibility owing to their hydrophilic character.

4. Conclusion

TiO₂ was synthesized by the sol-gel method using titanium butoxide as a precursor and doped with gold particles following the photodeposition method. Au-TiO₂ catalyst degraded the contaminant with percentages ranging from 88.6% for a concentration of 5 mg/L to 97.4% for a concentration of 30 mg/L, in a system irradiated with UV light. From LH-HW model evaluated, the experimental data have an adjustment to a first-order kinetics, which allows to obtain the values of the kinetic constants for the model, so it is concluded that LH-HW model describes the decomposition of the dye. The results by GC-MS support the fact of the degradation of the molecule, which means that there is not only a removal of the dye in solution, but also a rupture of bonds that results in the formation of the hydroxylated intermediates products to mineralize the molecule.

Conflicts of Interest

The authors declare no conflicts of interest regarding the publication of this paper.

References

- [1] Bethi, B., Sonawane, S.H., Bhanvase, B.A. and Gumfekar, S.P. (2016) Nanomaterials-Based Advanced Oxidation Processes for Wastewater Treatment: A Review. *Chemical Engineering and Processing-Process Intensification*, **109**, 178-189. <https://doi.org/10.1016/j.cep.2016.08.016>
- [2] Litter, M.I. (2005) Tecnologías Avanzadas de Oxidación. In: Blesa, M. and Blanco, J., Eds., *Solar Safe Water*, Universidad Nacional de General San Martín, Buenos Aires, 73.
- [3] Bora, L.V. and Mewada, R.K. (2017) Visible/Solar Light Active Photocatalysts for Organic Effluent Treatment: Fundamentals, Mechanisms and Parametric Review. *Renewable and Sustainable Energy Reviews*, **76**, 1393-1421. <https://doi.org/10.1016/j.rser.2017.01.130>
- [4] Rastogi, K., Sahu, J.N., Meikap, B.C. and Biswas, M.N. (2008) Removal of Methylene Blue from Wastewater Using Fly Ash as an Adsorbent by Hydrocyclone. *Journal of Hazardous Materials*, **158**, 531-540. <https://doi.org/10.1016/j.jhazmat.2008.01.105>
- [5] Chen, D., Zeng, Z.Y., Zeng, Y.B., Zhang, F. and Wang, M. (2016) Removal of Methylene Blue and Mechanism on Magnetic γ -Fe₂O₃/SiO₂ Nanocomposite from Aqueous Solution. *Water Resources and Industry*, **15**, 1-13. <https://doi.org/10.1016/j.wri.2016.05.003>
- [6] Ahmed, K.A.M. and Huang, K. (2018) Preparation, Characterization of CoxMn1-xO₂ Nanowires and Their Catalytic Performance for Degradation of Methylene Blue. *Journal of King Saud University- Science*, **30**, 49-56. <https://doi.org/10.1016/j.jksus.2016.11.004>
- [7] Postai, D.L., Demarchi, C.A., Zanatta, F., Rodrigues, A., Caroline, D. and Melo, C. (2016) Adsorption of Rhodamine B and Methylene Blue Dyes Using Waste of Seeds of *Aleurites moluccana*, a Low Cost Adsorbent. *Alexandra Engineering Journal*, **55**, 1713-1723. <https://doi.org/10.1016/j.aej.2016.03.017>
- [8] Adeleke, J.T., Theivasanthi, T., Thiruppathi, M., Swaminathan, M., Akomolafe, T. and Alabi, A.B. (2018) Photocatalytic Degradation of Methylene Blue by ZnO/NiFe₂O₄ Nanoparticles. *Applied Surface Science*, **455**, 195-200. <https://doi.org/10.1016/j.apsusc.2018.05.184>
- [9] Ameen, S., Akhtar, M. S., Kim, Y. S., Yang, O.-B. and Shin, H.-S. (2010) Synthesis and Characterization of Novel Poly (1-Naphthylamine)/Zinc Oxide Nanocomposites: Application in Catalytic Degradation of Methylene Blue Dye. *Colloid and Polymer Science*, **288**, 1633-1638. <https://doi.org/10.1007/s00396-010-2284-9>
- [10] Dhandapani, C., Narayanasamy, R., Karthick, S.N., Hemalatha, K.V, Selvam, S., Hemalatha, P. and Kim, H. (2016) Drastic Photocatalytic Degradation of Methylene Blue Dye by Neodymium Doped Zirconium Oxide as Photocatalyst under Visible Light Irradiation. *Optik*, **127**, 10288-10296. <https://doi.org/10.1016/j.ijleo.2016.08.048>
- [11] Rani, S., Aggarwal, M., Kumar, M., Sharma, S. and Kumar, D. (2016) Removal of Methylene Blue and Rhodamine B from Water by Zirconium Oxide/Graphene. *Water Science*, **30**, 51-60. <https://doi.org/10.1016/j.wsj.2016.04.001>
- [12] Mehrabian, M. and Esteki, Z. (2017) Degradation of Methylene Blue by Photocatalysis of Copper Assisted ZnS Nanoparticle Thin Films. *Optik*, **130**, 1168-1172. <https://doi.org/10.1016/j.ijleo.2016.11.137>
- [13] Basahel, S.N., Ali, T.T., Mokhtar, M. and Narasimharao, K. (2015) Influence of

- Crystal Structure of Nanosized ZrO₂ on Photocatalytic Degradation of Methyl Orange. *Nanoscale Research Letters*, **10**, Article No. 73.
<https://doi.org/10.1186/s11671-015-0780-z>
- [14] Djurišić, A.B., Leung, Y.H. and Ching Ng, A.M. (2014) Strategies for Improving the Efficiency of Semiconductor Metal Oxide Photocatalysis. *Materials Horizons*, **1**, 400-410. <https://doi.org/10.1039/C4MH00031E>
- [15] Gurushantha, K., Anantharaju, K.S., Sharma, S.C. and Nagaswarupa, H.P. (2016) Bio-Mediated Sm Doped Nano Cubic Zirconia: Photoluminescent, Judd—Ofelt Analysis, Electrochemical Impedance Spectroscopy and Photocatalytic Performance. *Journal of Alloys and Compounds*, **685**, 761-773.
<https://doi.org/10.1016/j.jallcom.2016.06.105>
- [16] Shumuye, D., Chandra, R. and Rao, S. (2017) Synthesis, Characterization and Visible Light Photocatalytic Activity of Mg²⁺ and Zr⁴⁺ Co-Doped TiO₂ Nanomaterial for Degradation of Methylene Blue. *Journal of Asian Ceramic Societies*, **5**, 136-143.
<https://doi.org/10.1016/j.jascers.2017.03.006>
- [17] Byrne, C., Subramanian, G. and Pillai, S.C. (2018) Recent Advances in Photocatalysis for Environmental Applications. *Journal of Environmental Chemical Engineering*, **6**, 3531-3555. <https://doi.org/10.1016/j.jece.2017.07.080>
- [18] Katouezadeh, E., Zebajad, S.M. and Janghorban, K. (2018) Synthesis and Enhanced Visible-Light Activity of N-Doped TiO₂ Nano-Additives Applied over Cotton Textiles. *Journal of Materials Research and Technology*, **7**, 204-211.
<https://doi.org/10.1016/j.jmrt.2017.05.011>
- [19] Joseane, J., Mesa, M., Ricardo, J., Romero, G., Carolina, Á., Macías, C. and Murcia, J.J. (2017) Methylene Blue Degradation over M-TiO₂ Photocatalysts (M = Au or Pt) Degradación de azul de Metileno Sobre Fotocatalizadores M-TiO₂ (M = Au o Pt). *Ciencia en Desarrollo*, **8**, 109-117.
<https://doi.org/10.19053/01217488.v8.n1.2017.5352>
- [20] Benzaouak, A., Ellouzi, I., Ouanji, F., Touach, N., Kacimi, M., Ziyad, M. and Lofti, E. M. (2018) Photocatalytic Degradation of Methylene Blue (MB) Dye in Aqueous Solution by Ferroelectric Li_{1-x}Ta_{1-x}W_xO₃ Materials. *Colloids and Surfaces A: Physicochemical and Engineering Aspects*, **553**, 586-592.
<https://doi.org/10.1016/j.colsurfa.2018.06.011>
- [21] Bensouici, F., Bououdina, M., Dakhel, A.A., Tala-Ighil, R., Tounane, M., Iratni, A. and Cai, W. (2017) Optical, Structural and Photocatalysis Properties of Cu-Doped TiO₂ Thin Films. *Applied Surface Science*, **395**, 110-116.
<https://doi.org/10.1016/j.apsusc.2016.07.034>
- [22] Mondal, S., De Anda Reyes, M.E. and Pal, U. (2017) Plasmon Induced Enhanced Photocatalytic Activity of Gold Loaded Hydroxyapatite Nanoparticles for Methylene Blue Degradation under Visible Light. *RSC Advances*, **7**, 8633-8645.
<https://doi.org/10.1039/C6RA28640B>
- [23] Houas, A., Lachheb, H., Ksibi, M., Elaloui, E., Guillard, C. and Herrmann, J.M. (2001) Photocatalytic Degradation Pathway of Methylene Blue in Water. *Applied Catalysis B: Environmental*, **31**, 145-157.
[https://doi.org/10.1016/S0926-3373\(00\)00276-9](https://doi.org/10.1016/S0926-3373(00)00276-9)
- [24] Torres, L. and Ruiz, M.A. (2011) Efecto del Dopaje de Indio y Níquel en la Propiedadestexturales, Estructurales y Catalíticas de Polvosnanométricos de Totania Preparado Por sol Gel. *Ciencia UANL*, **14**, 405-416.
- [25] Loddo, V., Bellardita, M., Camera-Roda, G., Parrino, F. and Palmisano, L. (2018) Heterogeneous Photocatalysis: A Promising Advanced Oxidation Process. In: A.

Basile, S. Mozia and R. Molinari, Eds., *Current Trends and Future Developments on (Bio-)Membranes*, Elsevier, Palermo, 1-43.

<https://doi.org/10.1016/B978-0-12-813549-5.00001-3>

- [26] Xi, Q., Han, S., Zhang, Q. and Zhao, D. (2018) Photocatalytic Oxidation Degradation Mechanism Study of Methylene Blue Dye Waste Water with GR/iTO₂. 2018 *International Conference on Novel Functional Materials*, Krakow, 20-24 August 2018, Vol. 238, Article No. 03006. <https://doi.org/10.1051/mateconf/201823803006>
- [27] Ray, S.K., Dhakal, D., Kshetri, Y.K. and Lee, S.W. (2017) Cu- α -NiMoO₄ Photocatalyst for Degradation of Methylene Blue with Pathways and Antibacterial Performance. *Journal of Photochemistry and Photobiology A: Chemistry*, **348**, 18-32. <https://doi.org/10.1016/j.jphotochem.2017.08.004>